Attosecond Science: Recent Highlights and Future Trends

Lukas Gallmann, Claudio Cirelli, and Ursula Keller

Physics Department, Eidgenössische Technische Hochschule Zürich, CH-8093 Zurich, Switzerland; email: gallmann@phys.ethz.ch

Annu. Rev. Phys. Chem. 2012. 63:447–69

First published online as a Review in Advance on January 30, 2012

The *Annual Review of Physical Chemistry* is online at physchem.annualreviews.org

This article's doi:
10.1146/annurev-physchem-032511-143702

0066-426X/12/0505-0447$20.00

Keywords

high-harmonic generation, attosecond spectroscopy, photoionization, tunneling, electron dynamics, ultrafast lasers

Abstract

We review the first ten years of attosecond science with a selection of recent highlights and trends and give an outlook on future directions. After introducing the main spectroscopic tools, we give recent examples of representative experiments employing them. Some of the most fundamental processes in nature have been studied with some results initiating controversial discussions. Experiments on the dynamics of single-photon ionization illustrate the importance of subtle effects on such extreme timescales and lead us to question some of the well-established assumptions in this field. Attosecond transient absorption, as the first all-optical approach to resolve attosecond dynamics, has been used to study electron wave packet interferences in helium. The attoclock, a recent method providing attosecond time resolution without the explicit need for attosecond pulses, has been used to investigate electron tunneling dynamics and geometry. Pushing the frontiers in attosecond quantum mechanics with increasing temporal and spatial resolution and often limited theoretical models results in unexpected observations. At the same time, attosecond science continues to expand into more complex solid-state and molecular systems, where it starts to have impact beyond its traditional grounds.

1. INTRODUCTION

Attosecond science: research field studying dynamical processes on attosecond (1 as = 10^{-18} s) timescales

XUV: extreme ultraviolet radiation

Attoclock: measurement technique employing intense nearly circular polarized laser pulses and angle-resolved momentum imaging to achieve attosecond temporal resolution

Strong-field interactions: nonperturbative, nonrelativistic laser-matter interactions at laser peak intensities ranging from $\sim 10^{13}$–10^{15} W cm^{-2}

2011 marks the tenth anniversary of attosecond science (1 as = 10^{-18} s). This research field was born with the first successful generation of ultrashort pulses of light (extreme ultraviolet, or XUV light, to be precise) with subfemtosecond duration (1, 2). Immediately following their availability, these pulses were applied to time-resolved studies of systems with transients of a few femtoseconds or less. But what dynamics do take place on an attosecond timescale? The orbital period of an electron in ground-state hydrogen in Bohr's model amounts to 150 as. The attosecond is thus the typical timescale for electronic motion on an atomic scale. The much higher inertia of atomic nuclei prevents them from exhibiting similarly fast dynamics under normal conditions. Their vibrational period in molecules is typically on the order of tens of femtoseconds and above. Femtosecond pulses are sufficiently short to enable taking molecular snapshots with the motion of the nuclei being frozen in most molecular systems (3). Attosecond pulses, on the other hand, permit snapshots of electronic motion.

The advance of time-resolved methods into the attosecond domain allows the experimentalists to ask entirely new questions. How long does it take to remove an electron from an atom or molecule (4–6)? How do the molecular orbitals rearrange after the sudden removal of an electron (7)? How and how fast do the electrons adapt to the moving potential landscapes during a chemical reaction? And a much more general and fundamental question: When is instantaneous a valid concept, and for what processes does such an assumption break down?

Some of the early experimental highlights in attosecond science include the lifetime measurement of inner-shell vacancies in Kr atoms (8), the direct sampling of the optical waveform of an ultrashort optical pulse in the time domain (9), the time-resolved observation of laser-induced tunnel ionization in atoms (10), and the recording of electron dynamics during photoemission from a tungsten surface (11). Throughout this first decade, the generation of attosecond pulses and their application to time-resolved studies have remained challenging. Even today, rather few research groups have a working attosecond spectroscopy setup in their laboratory.

In parallel to the development of methods employing single attosecond pulses to achieve the desired time resolution, alternative techniques yielding access to the attosecond domain have been devised. Core-hole clock spectroscopy was used to resolve the electron transfer from a sulfur adsorbate to a ruthenium surface (12). The so-called attoclock, on the other hand, utilizes the strong-field ionization induced by a nearly circular polarized laser pulse in combination with angle-resolved fragment detection to achieve the desired temporal resolution (13), whereas strong-field interactions with linearly polarized pulses were used to study proton dynamics in hydrogen and methane molecules (14). Interferometric techniques employing trains of closely spaced attosecond pulses not only reveal information about dynamics but also give access to quantum mechanical phase (5, 15).

These examples represent only a small selection of the work published during the first decade of attosecond science. However, they give an excellent cross-section of the topics of interest during these first years and show the promise that the field holds for addressing new questions in physics and chemistry. Indirectly, they also tell us what problems cannot yet be addressed by attosecond science and lead us to some of the major questions for the next decade in this area of research. From the point of view of enabling technology, we need to find spectroscopic techniques that can be more easily applied to more general systems. Many of the previous experiments were rather governed by the need to find suitable systems that can be studied with a given approach than the other way round. Simultaneously, the generation of attosecond pulses must become easier to allow a wider group of researchers to gain access to attosecond tools. From the point of view of science, two major directions drive research in the field on the threshold of its next decade. On one side, there is a great

effort to extend attosecond science to more complex molecular or solid-state systems. On the other side, attosecond tools now allow the experimenter to investigate some of the most fundamental aspects in physics and chemistry and even to question some long-standing assumptions.

Several excellent review articles have been written about attosecond science in the past (16–22). In this paper, we thus focus on the major trends and developments during the last few years. It is our goal to provide a self-contained and self-consistent view of the field. Partial overlap with previous articles is thus unavoidable but is kept at a minimum. Our reference point is an earlier article on attosecond electron dynamics by Kling & Vrakking (21) that appeared in 2008 in the *Annual Review of Physical Chemistry*.

Our paper is organized as follows: In the next section, we give an overview on the experimental tools in attosecond science. As they have been described in detail in other review articles, we only briefly cover the generation of attosecond pulses and the traditional attosecond spectroscopy techniques. We emphasize two new techniques that have emerged in recent years. One is the so-called attoclock that achieves attosecond resolution and timing accuracy without the need for attosecond pulses (13). The other is attosecond transient absorption spectroscopy (23–25), which is a very well-established method in other regions of the electromagnetic spectrum and/or on longer timescales. The power of this all-optical approach is illustrated with an experiment on interfering, transiently bound electron wave packets in helium.

After introducing the attosecond spectroscopy tools, we review recent progress on hot topics in the field. Attosecond science has begun to ask more and more fundamental questions. One such question that recently raised particular attention is, How long does it take to remove an electron from an atom? This question has been addressed with different techniques and for various ionization processes. Experiments discussed in more detail also demonstrate the power of the attoclock technique. We then conclude with an outlook on future perspectives.

Attosecond transient absorption: measurement technique using attosecond pulses to probe induced changes in optical absorption

HHG: high-harmonic generation

2. ATTOSECOND SPECTROSCOPY TECHNIQUES

Strong-field laser matter interactions are an ingredient of every present attosecond experiment in one way or another. Strong field usually refers to laser peak intensities on the order of 10^{13}–10^{15} W cm^{-2}. Such intensities correspond to the electrical field that represents an ultrashort laser pulse reaching field strengths comparable to inner-atomic fields. As a result, the laser field becomes capable of ionizing atoms even if the photon energy amounts to only a small fraction of the ionization potential. The upper limit to the intensity range defining the strong-field regime is usually given by the onset of relativistic effects in the laser-matter interaction. Although the generation of rather energetic attosecond pulses is also predicted for the relativistic regime (26–28), we restrict our discussion to the nonrelativistic case.

It is clear that with such high field strengths, the laser field cannot be considered a perturbation to an atom or molecule anymore. A prototype physical process that occurs under such conditions is high-harmonic generation (HHG) (29–34). In HHG, an intense laser beam is focused into an atomic or molecular gas target. The electric field inside the laser pulse is strong enough to ionize the target gas. The liberated electron is subsequently accelerated in the laser field. As the oscillating electric field vector of the laser pulse reverses its direction, the electron is slowed down and eventually driven back to its parent ion. The electrons that return to their ion may recombine with finite probability. Upon recombination, excess kinetic energy is emitted as an energetic photon. This simple quasi-classical description of the process is known as the three-step model and was originally introduced in 1993 by Corkum (33). It is schematically depicted in **Figure 1*a***.

When looking at the classical trajectories of the electrons in the external electric field of the driving laser pulse, one finds that electrons released between the zero-crossing and maximum

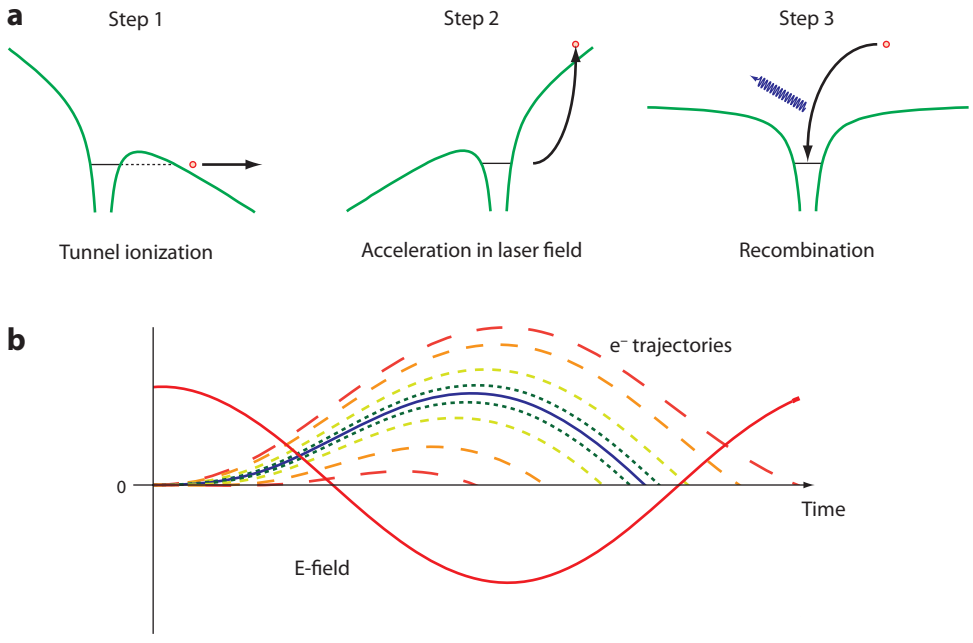

Figure 1

High-harmonic generation (HHG). (*a*) The semiclassical three-step model of HHG. The atom is ionized by the strong laser field (step 1). The liberated electron is subsequently accelerated in the oscillating field (step 2). Some electron trajectories recollide with the parent ion. Recombination may occur with the emission of a high-harmonic photon (step 3). (*b*) Classical electron trajectories of the liberated electron in the external laser field. Only trajectories leaving the atom during the first quarter-cycle after a field maximum recollide. The color code of the trajectories illustrates the recollision energy of the electron, with blue representing the highest (so-called cut-off) energy.

amplitude of the field never return to the parent ion. Those electrons do not contribute to HHG. Electrons freed between the field maximum and its next zero-crossing, however, return to the parent ion and may recombine (**Figure 1*b***). The actual trajectory and the energy gained by the electron depend on its release time. This temporal confinement of HHG results in an attosecond temporal structure of the emitted pulses of high-harmonic radiation.

There are two important regimes for attosecond pulse generation. If long pulses (i.e., pulses lasting many oscillation cycles of the electrical field) are used to drive the HHG process, a train of attosecond pulses is created (1). This is because the process described above and depicted in **Figure 1** is periodically repeated for each half-cycle of the electric-field oscillations. The attosecond pulse train (APT) therefore consists of pulses separated by half the oscillation period. On a longer timescale, the APT follows an envelope that is somewhat shorter than the driving laser pulse. The quasi-periodic structure of the APT results in a comb of evenly spaced odd harmonics of the original laser frequency in the spectral domain.

If the three-step process can be limited to a single occurrence during a driving laser pulse, the regime of single or isolated attosecond pulse (IAP) generation is reached (2). Because of the missing periodicity, the spectral signature of isolated attosecond pulse production is a continuum of emitted photon energies. The high-harmonic emission can be constrained to a single half-cycle of the laser pulse by applying an appropriate gating mechanism. The most straightforward and oldest approach is to use the shortest possible laser pulse (2). In this case, the laser pulse needs

Attosecond pulse train (APT): generation of multiple attosecond bursts of radiation per driving infrared laser pulse

Isolated attosecond pulse (IAP): generation of one attosecond burst of radiation per driving infrared laser pulse

to be short enough to contain only one half-cycle that reaches sufficiently high field strength to create the high-harmonics of interest. Not only the first isolated attosecond pulses but also the shortest pulses to date have been generated with this method (35). 3.3-fs laser pulses at a center wavelength of 720 nm (1 cycle = 2.4 fs) were used to produce 80-as pulses centered at a photon energy of ~80 eV. However, because the generation of such intense near-single-cycle laser pulses poses a major challenge, alternative approaches to IAP production have been devised that lead to considerably relaxed constraints on the driving laser. Because the recollision step of the three-step model can occur for only linear or very close to linear laser polarization, a clever polarization modulation scheme can be used to limit the high-harmonic emission to a single recollision event (36, 37). Combining this technique with an additional modulation of the electric-field oscillations by admixing the second-harmonic of the laser field has led to the generation of IAP from laser pulses as long as 28 fs (38). Another effect that can be used to limit high-harmonic emission to a single half-cycle is the depletion of the generating medium. If the instantaneous laser intensity reaches above a certain value, most of the gas in the target volume will be ionized and thus cannot participate in the three-step process anymore. Already at lower intensities, the creation of free electrons can dephase the high-harmonic radiation from the driving laser pulse and effectively shut off HHG. The corresponding ionization gating technique is another approach that has led to the successful generation of IAP (39, 40). The most energetic isolated attosecond pulses to date with a pulse energy of 2.1 nJ on target, a duration of 155 as, and a center photon energy of ~25 eV have also been generated with this method (41).

How can we apply these pulses to resolve attosecond dynamics? The traditional way in ultrafast spectroscopy in the femtosecond domain is the pump-probe approach. The pump pulse initiates a process, whereas the probe pulse measures the induced change in an optical observable after a certain delay with respect to the pump. If the physical effect being studied is repeatable, one can observe the full dynamics of the system by scanning the delay between the two pulses. The origin of the signal must be at least a two-photon process as the measured signal depends on both the pump and the probe pulse. To make maximum use of the temporal resolution offered by the ultrashort pulse, one usually derives the pump and the probe from the same initial laser pulse, thereby assuring perfect synchronization. If the pump-probe signal indeed results from a two-photon process, then the instantaneous signal power depends on the square of the instantaneous laser power (or of a higher power for a higher order process). Can this traditional scheme be transferred into the attosecond domain? A simple signal-level consideration shows why this is not presently possible (42): Pump-probe spectroscopy in the femtosecond domain is typically performed with nanojoule pulse energies at 100 MHz repetition rates. In attosecond science, we have access to only nanojoule pulse energies at repetition rates on the order of 1 kHz. This fact alone already results in a drop of signal levels by five orders of magnitude. But even worse, cross-sections for multiphoton interactions in the XUV spectral region where the attosecond pulses are located are considerably lower than in the visible or near-infrared (IR), where the femtosecond lasers operate. As a result, today's methods of choice that rely on attosecond pulses to achieve temporal resolution use the interaction of a strong, femtosecond visible/near-IR laser field with the attosecond pulse in the target. The intense femtosecond beam boosts signal levels in this two-color scheme to acceptable levels.

Below, we give a detailed description of the most successful attosecond spectroscopy techniques in use today. **Figure 2** gives a schematic overview of the three methods being discussed. The attosecond streak camera using a linearly polarized laser pulse in conjunction with the attosecond pulse is the oldest approach (2, 43). We also describe closely related (in terms of experimental setup) methods that are employed in experiments with APTs (1, 15, 44, 45). As pointed out in the introduction to this review, both APTs and IAPs have been used to investigate attosecond

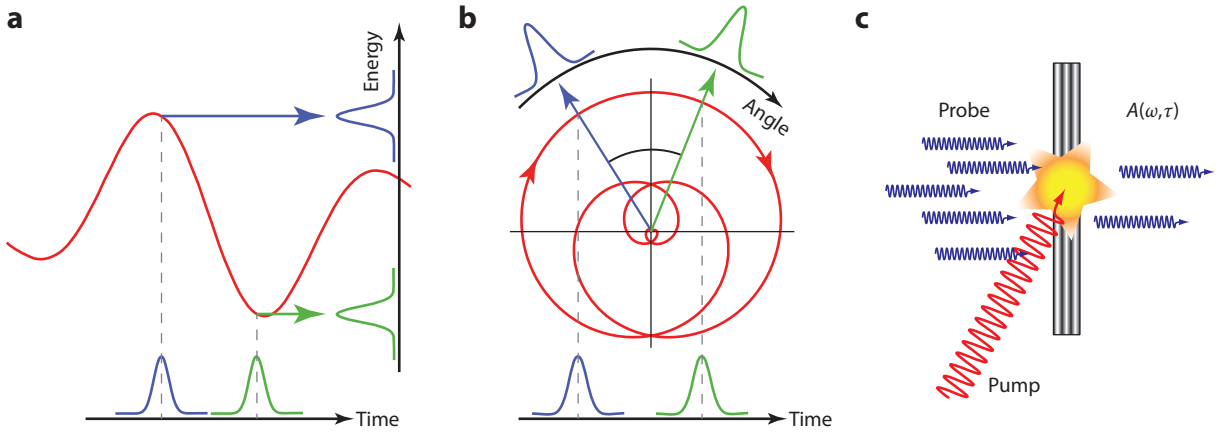

Figure 2

Schematic functional principle of the presently most common attosecond spectroscopic techniques. (*a*) Attosecond streak camera. Interaction with a streaking laser field (or vector potential) maps electron wave packets created at distinct times to different final energies or momenta. The RABBITT technique can be understood in the time domain as a periodic version of this process. (*b*) Attoclock. Through interaction with a nearly circular polarized laser field, events separated in time are mapped to different angles in the final momentum distribution. (*c*) Attosecond transient absorption. A pump pulse modifies the absorption properties of the sample. These modifications are probed with the attosecond pulse as a function of photon energy and delay with respect to the pump. Abbreviation: RABBITT, reconstruction of attosecond harmonic beating by interference of two-photon transitions.

dynamics in various systems. Alternative schemes relying solely on strong-field interactions to achieve attosecond time resolution have also been demonstrated. A rather recent member of this category is the attoclock, or attosecond angular streaking (13), which is capable of resolving attosecond dynamics without requiring attosecond pulses. Even more recent is the first generally applicable all-optical approach to attosecond time-resolved spectroscopy. In 2010, the transient absorption technique that is well established in the femtosecond domain has been transferred to attosecond science (23–25). With transient absorption, one detects the probe beam transmission through an optical medium as a function of pump-probe delay.

2.1. Attosecond Streak Camera and Related Approaches

The attosecond streak camera concept was initially introduced for characterizing isolated attosecond pulses (2, 43). Soon thereafter, the same approach was applied to perform actual time-resolved spectroscopy experiments [see, e.g., (4, 6, 8–11, 13)]. The principle of streaking can be divided into two individual steps. In a first step, an initially bound electron is near-instantaneously liberated, e.g., by an isolated attosecond pulse. In the second step, it is accelerated by the streaking laser field. The streaking dynamics can very often be treated semiclassically. For the attosecond streak camera, a linearly polarized laser field (typically in the IR spectral region) is used both as the streaking field and as the generation field for the attosecond pulse. This assures perfect synchronization between the two pulses. The detected electron momentum (or energy) distribution experiences a shift that depends on the relative timing between the liberation event and the laser pulse. Thereby, time is mapped to momentum or energy. If recorded over a range of delays, one essentially measures a cross-correlation between the created electron wave packet and the electric field of the laser. As this measurement depends on the electric field of the pulse rather than its envelope, one attains subfemtosecond resolution despite cross-correlating with a multifemtosecond pulse. Under

suitable conditions, one can then extract information about the dynamics of the system under study from these cross-correlation data. Usually, one analyzes the streaking traces at different electron energies. A phase shift between the streaking traces recorded at two given electron energies (e.g., corresponding to two different initial atomic or molecular states) can be interpreted as a time delay in emission of the electrons from the target. For a more detailed description of the attosecond streak camera, the reader is referred to one of the earlier reviews on attosecond science (e.g., 21).

The experimental implementation of the attosecond streak camera for a given system to be investigated can be rather challenging—in addition to the significant difficulties already involved in the generation of isolated attosecond pulses. The streaking field can generate a significant background signal through above-threshold ionization. It is often tedious work to find proper operation parameters that allow extracting the actual streaking signal from such a background. This is usually all the more demanding the smaller the energy of the electrons one wishes to detect and the lower the ionization threshold of the target.

Concepts very similar to the attosecond streak camera in terms of the underlying physics and experimental setup are also used with APTs. Reconstruction of attosecond harmonic beating by interference of two-photon transitions (RABBITT) (1, 44) is a measurement technique that is specialized on the characterization of APTs. In its most common implementation, it measures the relative phase of the individual harmonics forming the APT, or equivalently, the average shape of the attosecond pulses within the pulse train, neglecting pulse-to-pulse variations. However, the spectral phase information contained in the RABBITT data can also give insight into attosecond dynamics. In particular, attosecond processes underlying HHG in simple molecules such as CO_2 and N_2 were investigated with RABBITT (46–48). The interference of angularly resolved photoelectron spectra from consecutive pulses in the APT under the influence of a streaking field allowed the reconstruction of the phase information of the electron wave packets initiated by the individual attosecond pulses (15). In a similar experiment, the sequence of pulses in the APT acted like a stroboscope, resolving single ionization events in argon and helium (45).

RABBITT: reconstruction of attosecond harmonic beating by interference of two-photon transitions

CEP: carrier-envelope offset phase

2.2. Attoclock

A completely different approach is exploited in attosecond angular streaking, i.e., the attoclock (13). Here, measuring time is achieved by counting cycles, as is done on a watch face: During one hour, the minute hand of a watch completes one cycle and maps time to angle univocally. The analogous action in strong-field ionization is achieved by employing close-to-circularly polarized laser pulses: The electric field vector—while rotating in the polarization plane—ionizes and further deflects the electrons in the spatial direction perpendicular to the field propagation, such that the instant of ionization is mapped to the final angle of the momentum vector in this plane. Hence, time is mapped to angle.

This attoclock runs over 360° within one optical cycle that takes ~2.7 fs for a laser pulse centered at 800-nm wavelength. Measuring the emission angle of the electron enables one to measure time with a precision well below one optical period. One degree of angular resolution corresponds to 7.4 as at a center wavelength of 800 nm. In principle, there is no fundamental lower limit, because electron momentum vectors can be measured with very high precision. The attoclock provides this attosecond timing information without requiring attosecond pulses. Interestingly, the idea of angular streaking had already been proposed theoretically in 2000 as a single-shot method to measure the carrier-envelope offset phase (CEP) (49) of few-cycle pulses (50). The CEP is the relative phase between the envelope of an ultrashort laser pulse and its carrier wave. The additional potential of angular streaking to retrieve timing information was not envisioned in 2000 and became clear only after the realization of the first measurements.

The first experiment introducing the attoclock technique was realized by measuring the ion momentum distribution of helium that was tunnel-ionized by phase-controlled, nearly circular polarized laser pulses in the two-cycle duration regime (13). While keeping the pulse peak intensity constant, the CEP was varied, thereby controlling the azimuthal direction of the maximum electric-field vector, which eventually determines the predominant direction for the ionized electrons.

The magnitude of the electric-field maximum does not depend on the CEP in the case of perfectly circular polarized pulses. However, it is technically difficult to generate such pulses in the few-cycle regime because of their large spectral bandwidth. A residual amount of ellipticity results in subcycle oscillations on the electric field magnitude, which therefore exhibit a CEP dependence (the rapid oscillations move with varying CEP).

These oscillations become the dominant feature in tunnel ionization experiments owing to the high nonlinearity of the process. According to theory, the rate of tunnel ionization obeys the following trend (51):

$$W_{TI} \propto \exp\left(-\frac{2(2I_p)^{3/2}}{3E}\right), \quad (1)$$

where I_p is the ionization potential and E the nonadiabatic electric field amplitude.

From Equation 1, we see that it is enough to vary the electric field amplitude E by 10% (from 0.1–0.09 a.u.) to reduce the ionization rate by almost one order of magnitude, while keeping all the other parameters constant.

With elliptically polarized pulses, the electric-field amplitude oscillates in an optical cycle between local minima (where the ionization rate is strongly suppressed) and local maxima (where the rate is enhanced). This is illustrated in **Figure 3*a***. The result is that the radially integrated momentum distributions show two distinct peaks separated by ~180°, whose relative intensity change while varying the CEP. The role of the CEP is to shift the rapid oscillations of the electric-field magnitude under the pulse envelope. When the electric-field maximum points in the direction of the major axis of the polarization ellipse, one peak dominates the other. But when the CEP is changed by $\pi/2$, the electric field points in the direction of the minor axis of the ellipse, and two smaller peaks of equal height are created.

The experimental data shown in **Figure 3** were obtained with a cold-target recoil-ion momentum spectrometer (52). The data were reproduced extremely well by a semiclassical model (33, 53) based on strong-field tunnel ionization and subsequent classical propagation. By comparing data and simulations, a temporal localization accuracy of 24-as rms was demonstrated, and a time resolution of ~200 as was estimated. Besides providing a direct measurement of the CEP with an accuracy of ~60 mrad, the first quantity indicates how precisely timing information can be extracted using the attoclock, whereas the second represents the minimum time difference that still allows separation of two ionization events.

The attoclock is a powerful technique that can rely solely on strong-field interactions with the sample to resolve attosecond dynamics. In Sections 4.2 and 4.3, we give a detailed discussion of two applications of the attoclock to study fundamental physics during ionization processes.

2.3. Transient Absorption

The streaking methods have been by far the most successful and most versatile approaches to attosecond time-resolved spectroscopy demonstrated so far. However, they have in common a number of inherent weaknesses and limitations. First, the intrinsically required strong laser field distorts the system under testing. Then, all streaking methods detect charged particles, which limits measurement speed and signal-to-noise ratio. Schemes relying on electron detection are particularly susceptible to space-charge effects and distortions. Furthermore, the strong laser

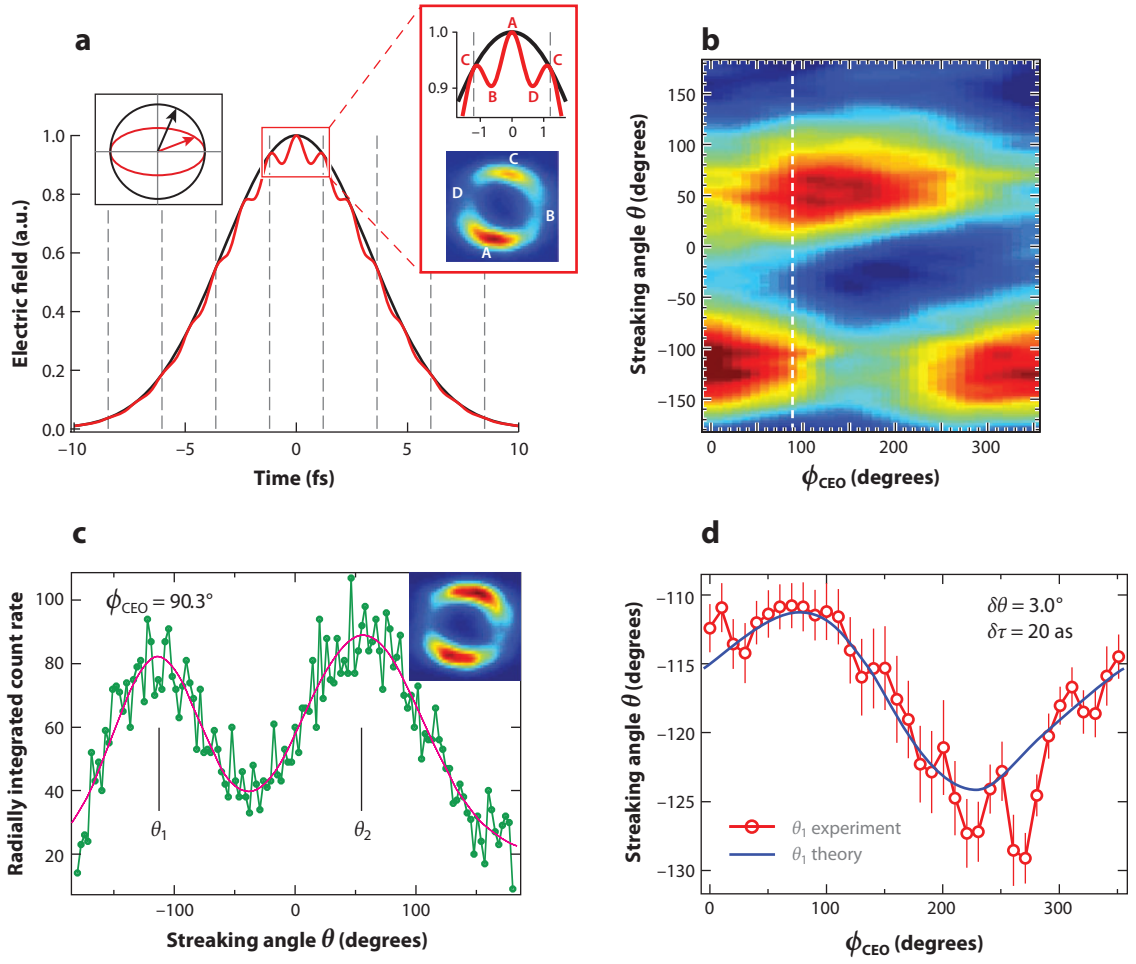

Figure 3

Attoclock with elliptically polarized light. (*a*) Magnitude of the electric field as a function of time for light with perfect circular polarization (*black*) and elliptical polarization (*red*; $\varepsilon = 0.92$) for CEP $= 0$. The dashed lines indicate the optical cycles (2.42 fs for 725-nm central wavelength). The inset on the left illustrates how the electric field vector rotates along a circle (*black*) for circular polarization or along an ellipse (*red*) for elliptical polarization. The inset on the right shows that within the central optical cycle (where most of the ionization takes place), the electric-field magnitude peaks at two instants in time labeled A and C and reaches local minima at other instants labeled B and D. This evolution manifests itself directly in the momentum distribution. (*b*) Radially integrated momentum distributions of helium ions obtained while scanning the CEP over 2π. (*c*) Linear cut at CEP $= \pi/2$ (marked in panel *b* with a white dashed line) showing the two-peak structure. (*d*) Angular position θ_1 of one of the two peaks obtained by a double-Gaussian fit, as shown in panel *c*, plotted as a function of CEP (*red*: data; *blue*: simulations). Comparing the data with a simulation based on a semiclassical model allows the estimation of the temporal localization accuracy. Abbreviations: CEO, carrier-envelope offset; CEP, carrier-envelope offset phase.

field can create a significant background of electrons through strong-field ionization processes. Although the streaking techniques will be difficult to replace for certain applications in attosecond science, it remains questionable how well they are transferrable to systems exhibiting complex dynamics.

A new measurement method that was reported for the first time in 2010 for the attosecond domain holds promise to address some of the major shortcomings of the streaking techniques

EWPs: electron wave packets

and gives access to additional physical observables (23). This new and purely optical method is called attosecond transient absorption (23–25, 54, 55). Transient absorption is a well-known and well-established measurement technique in the femtosecond domain (see, e.g., References 56, 57 for transient absorption with high-harmonic sources) but was only recently extended into the attosecond regime using isolated attosecond pulses (23). Transient absorption measures the probe pulse spectrum transmitted through the sample as a function of pump-probe delay. In transient absorption spectroscopy, there is no intrinsic need for the presence of a strong laser field, and it relies on the detection of photons. Photons do not suffer from space-charge effects, are insensitive to stray electric or magnetic fields, and can be detected very efficiently, sensitively, and with high dynamic range using existing charge-coupled device technology. In our laboratory, we found that for comparable experimental parameters, we gain approximately two orders of magnitude in measurement time (6 min versus 10 h) for a full pump-probe scan when using transient absorption rather than conventional electron detection using a simple time-of-flight spectrometer. Such a reduction in measurement time is a prerequisite for certain experiments, where samples may contaminate/oxidize/degrade in a short time, even under vacuum. Transient absorption allows selective probing of transitions and resonances. In addition, streaking methods intrinsically involve ionization in one way or another, whereas transient absorption is capable of directly probing bound-bound transitions. Because of the high sensitivity of the method, transient absorption spectroscopy is also expected to be a promising route toward true attosecond pump–attosecond probe experiments, a holy grail presently out of reach for existing attosecond technology. It also needs to be stated that transient absorption does probe a fundamentally different physical observable in a time-dependent system than do the traditional schemes based on ionization and may thus provide additional, otherwise inaccessible, information (25).

Two transient absorption experiments have been performed so far that involve isolated attosecond pulses. The first experiment observed electron wave packet motion in the valence shells of krypton ions (23). Soon thereafter, attosecond transient absorption was applied to time-resolve autoionization of argon atoms (24). Transient absorption spectroscopy also works well with APTs. We were the first to demonstrate this new technique with APTs and reported the only transient absorption experiment observing subfemtosecond dynamics to date (25). To give a practical example of attosecond transient absorption spectroscopy, we present this experiment in the following section. Despite the few experiments performed so far with attosecond transient absorption, this technique has great potential and can be expected to become a standard spectroscopic tool as transient absorption is in the femtosecond domain since decades.

3. WATCHING ELECTRON WAVE PACKETS INTERFERE

APTs allow for probing the interference of electron wave packets initiated by the individual pulses in the train (15, 45, 58). The interference of subsequent wave packets enhances the sensitivity of the method and enables the extraction of phase information. Recently, the ionization probability of helium atoms with APT photon energies below the ionization threshold in the presence of a time-delayed IR field was studied (58). The IR intensity on the order of 10^{13} W cm^{-2} was chosen not to induce strong-field processes in ground-state helium on its own. It was found that the ion yield is modulated with twice the IR driving laser frequency. The result was explained by the interference of transiently bound electron wave packets (EWPs). We investigated this physical system with attosecond transient absorption spectroscopy to gain more direct insight and to confirm this explanation.

The mechanism underlying the transiently bound EWP interference is schematically depicted in **Figure 4*a***. The atomic potential is deformed by the oscillating IR field. This modifies the

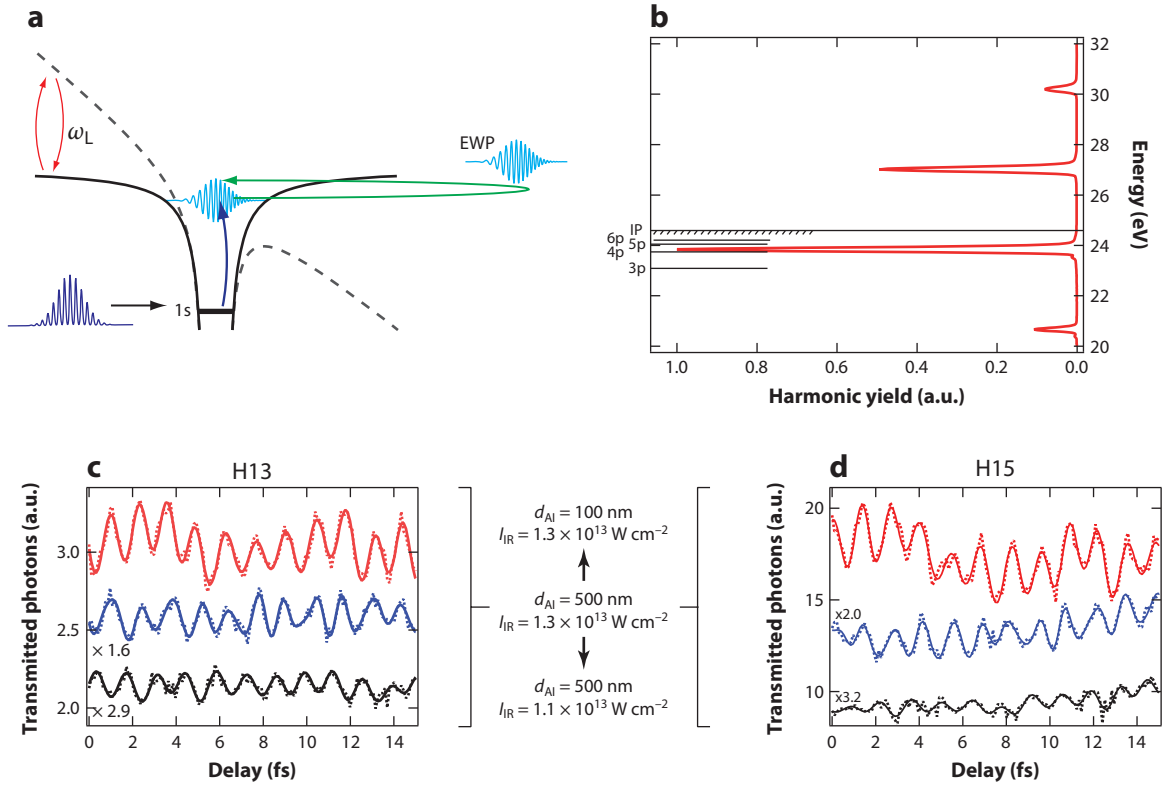

Figure 4

Interference of transiently bound electron wave packets. (*a*) An incoming attosecond pulse contained within an attosecond pulse train (APT) excites an electron wave packet (EWP), which is subsequently accelerated by the external laser field. The EWP returns to the parent ion at the instant the next pulse in the APT excites a new wave packet. As the entire process is coherent, interference will occur. (*b*) Energetic configuration of the experiment. The p-levels of helium directly accessible through absorption of a single extreme ultraviolet (XUV) photon are indicated on the left. The harmonic spectrum of the APT is shown on the right (*red solid line*). The field-free ionization threshold of helium is marked with a horizontal solid black line. (*c*) Photon yield of harmonic 13 transmitted through the helium target as a function of infrared (IR)-APT delay. The modulations are compared for different aluminum filter thicknesses changing the spectral phase between neighboring harmonics and for different IR intensities. Only the latter results in a phase shift of the modulations. (*d*) Same as in panel *c* but for harmonic 15.

absorption probability for the APT photons as a function of relative delay between the two fields. The energetic configuration of the experiment in **Figure 4*b*** shows the location of the individual harmonics forming the APT in relation to the ionization threshold of helium. It becomes clear that the EWPs are only transiently bound because the potential barrier may be sufficiently lowered for proper delay between the IR and the APT such that the wave packets can escape into the continuum. The EWPs accelerated by the IR field have returned with a certain probability back into the vicinity of the ion when a subsequent attosecond pulse excites the next wave packet. These processes obey a half-cycle periodicity owing to the symmetry of the system. The interference between wave packets excited by subsequent attosecond pulses significantly alters the ionization probabilities with delay. It is found that this interference effect dominates the modulation of the absorption through deformation of the atomic potential by an order of magnitude (58).

In the theoretical part of their study, Johnsson et al. (58) found that only 60–70% of the population transferred out of the ground state by the XUV is ionized in the presence of the IR field,

whereas ~30–40% of the population promoted by the XUV remains in an excited state. Because the detection of He^+ ions is only sensitive to processes leading to the ionization of an atom, it gives only incomplete information on the dynamics of this experimental system. This is a clear example in which transient absorption spectroscopy yields more insight than the traditional photoelectron- or photoion-detection-based methods. As shown in **Figure 4*c*,*d***, attosecond transient absorption not only provides the time-resolved ionization probability but also measures the spectrally resolved absorption probabilities. When comparing the transmitted photon yield modulations at the different harmonics forming the APT, one observes that they are not necessarily in phase with respect to each other. Our experiments have shown that the relative phase of these modulations does not depend on the relative optical phase between the different high harmonics. However, it reacts very sensitively to a change of the IR intensity. This observation qualitatively confirms the model introduced by Johnsson et al. (58) in a more rigorous way than initially possible with the He^+ experiment. The optical phase between the different harmonics maps to a temporal phase that is identical for all the EWPs. It therefore plays no role for the interference condition between subsequent wave packets. A change in the IR intensity, however, modifies the quantum mechanical phase accumulated by a transiently bound EWP during its excursion into the continuum (59, 60). When the returning EWP interferes with the EWP just excited by the subsequent pulse in the APT, this contribution governs the relative phase and, thus, decides between constructive or destructive interference.

The EWP interference picture is further confirmed by independent theoretical approaches. Rivière et al. (61) introduced a minimal analytical model for the total photon absorption probabilities based on the strong-field approximation. In their model, the modulation of the absorption probability is assigned exclusively to the interference of electron wave packets. An alternative theoretical description based on Floquet theory arrives at similar conclusions (62).

In a fraction of the time needed for a traditional experiment detecting photoelectrons or ions, we acquired data with excellent signal-to-noise ratio and without compromise on temporal and spectral resolution. Most theoretical tools in attosecond and strong-field science are geared toward computing ionization yields rather than the optical properties of a particular interaction. Only a few theoretical papers on transient absorption in the attosecond domain exist (54, 55). A significant effort is therefore also needed toward developing the new theoretical frameworks for transient absorption in the attosecond domain. In combination with an improved theoretical understanding, attosecond transient absorption holds great promise as a spectroscopic tool in attosecond science.

4. EXPLORING FUNDAMENTAL PHYSICS QUESTIONS

The investigation of ionization dynamics has been a major ongoing topic in attosecond science. The reason for this is not only rooted in the fundamental importance of ionization processes in nature but also in the operation principle of attosecond spectroscopic techniques. The attosecond streak camera and the attoclock intrinsically involve ionization (see Sections 2.1 and 2.2). It is thus a rather self-evident move to apply these methods to study ionization physics. Indeed, the earliest attosecond experiments were already exploring ionization dynamics (8). However, a clear trend in attosecond science can be observed. Whereas the first experiments were investigating systems with timescales and behavior rather well-known, either from spectroscopic data (8, 63) or from well-established theory (10, 64), recent studies attend to processes with unknown dynamics, e.g., the photoemission from a solid-state surface (11), strong-field ionization (6), or single-photon ionization (4, 5). The latter effect is conventionally assumed to occur even instantaneously—in conflict with the reports from the latest experiments. On the verge of its next decade, we thus witness a transition of attosecond science from proof-of-principle experiments primarily

demonstrating and testing the tools to new experimental findings truly addressing some of the most fundamental questions in physics.

In the following sections, we discuss the most recent studies of ionization dynamics in more detail. Section 4.1 covers the measurement of a relative time delay in the photoemission from two different energy levels in neon and argon, whereas Section 4.2 reports on the observation of a finite delay time in tunnel ionization. An application of the "hour hand" of the attoclock to investigate the importance of electron correlations in double ionization with close-to-circular polarized laser pulses is discussed in Section 4.3.

4.1. Time Delay in Photoemission

Single-photon ionization is one of the most fundamental processes in nature. Whether this process occurs instantaneously or takes a finite amount of time is therefore of prime interest. As an electron is removed from an atom, the remaining electrons will have to rearrange onto the new energy levels of the ion. How fast can such concerted motion of multiple electrons happen? Can we learn something about electron correlations in atoms from such dynamics? Furthermore, it has been suggested to use atomic reference states to obtain absolute timing information in streaking experiments (65). For this purpose, knowledge about a possible time delay in photoemission is indispensable. Two recent experiments have investigated the dynamics of single-photon ionization in neon and argon (4, 5).

A first experiment investigating a possible time delay in photoemission used isolated attosecond pulses centered at 106 eV and with a duration below 200 as together with the attosecond streak camera (4). Electrons released from the 2s and 2p orbitals of neon by this attosecond pulse are well separated in energy. Liberating them in the external streaking field thus leads to two distinct streaking traces at different mean electron kinetic energies. A phase difference between the oscillating streaking patterns relates to a time delay in the emission from the two atomic energy levels. In Reference 4, a more precise approach was chosen by extracting the delay information from the reconstructed phase of the two streaked electron wave packets. The reconstruction algorithm is an adapted version of the frequency-resolved optical gating algorithm known from ultrashort optical pulse characterization (66). By this method, it was found that the electron wave packet emitted from the 2p state lags approximately 20 as behind the one from the 2s state (4). Varying the amplitude of the streaking field by a factor of 6 did not have a noticeable effect on the measured delay time. Other authors, however, stress that interaction of the outgoing wave packets with the Coulomb potential and the streaking field may mimic a time delay in the streaking traces depending on the system being studied and the photon energy of the attosecond pulse (67–70).

The relative timing of photoemission from the $3s^2$ and the $3p^6$ shells of argon was investigated with APTs and the RABBITT (Section 2.1) technique (5). In analogy to the previous example employing isolated attosecond pulses, the delay is extracted from the electron wave packet phase measured with RABBITT. The authors show that the influence of the measurement process needs to be taken into account even when it involves only the relatively weak IR laser fields of the RABBITT method (5). In fact, the influence of the IR laser field is even the dominating contribution in their experiment. However, it can be taken into account with a proper theoretical model. After subtracting the contribution by the laser field, it is found that the p-electrons are emitted ~20 as after the s-electrons at excitation energies of 37 and 40 eV.

It needs to be pointed out that the precision of the measurement does not depend on the duration of the attosecond pulses for either experiment measuring the time delay in photoemission (4, 5). It rather depends on the accuracy with which one can extract the phase information from the measured data. Error sources for the phase reconstruction can be as diverse as the mechanical stability of the setup, signal-to-noise ratio of the data, delay, and energy calibration.

Although more experimental and theoretical work is needed for a proper understanding of photoemission from atoms and molecules, the two experiments presented in References 4 and 5 impressively demonstrate that attosecond tools are capable of resolving some of the fastest dynamics and thereby addressing entirely new problems in fundamental physics.

4.2. Tunneling Delay

The excellent temporal localization accuracy offered by the attoclock technique (Section 2.2) opened the possibility to study another fundamental aspect of quantum mechanics: the ability of particles to pass classically forbidden regions by tunneling through a barrier. It is commonly accepted that a strong laser field deforms the binding potential of an atom so strongly that a potential barrier is created through which an electron may tunnel (**Figure 1*a***). This is the principle of strong-field tunnel ionization, which was proposed by Keldysh (64) almost 50 years ago. However, a direct measurement of a hypothetical traversal time needed for the electron to tunnel through such a potential barrier or a precise estimation of the instant of ionization was never realized.

The attoclock technique appears to be ideally suited for such a measurement: A real and measurable tunneling delay time would manifest itself in an angular offset of the entire momentum distribution. The main challenge lies in the fact that a measurement of an angular offset, and the subsequent calculation of an absolute delay time, assumes the knowledge of the absolute angular position of the electric field maximum at the instant of ionization. In the case of perfectly circular polarized light, the only way to determine the instantaneous direction of the maximum electric field vector is an independent measurement of the CEP, performed for instance with the so-called stereo–above threshold ionization method (71–73). In the case of elliptically polarized pulses, however, it is the orientation of the ellipse (which remains fixed in space) that provides the reference for the electric-field orientation, without the need for determining or locking the CEP (6). A polarimetry measurement returns the orientation of the polarization ellipse in the laboratory frame.

An electron that exits the tunnel barrier, at the instant t_0, is driven by the electric field $E(t)$ of the laser pulse and is detected with a final momentum $p(t_0) = -A(t_0)$ [atomic units are used throughout this article], where $A(t_0)$ is the rotating vector potential of the elliptically polarized pulse, defined as

$$A(t_0) = \int_{t_0}^{\infty} E(t')dt'. \tag{2}$$

A real traversal time for tunneling Δt_D would manifest itself as an angular offset because the final electron momentum would be given by $-A(t_0 - \Delta t_D)$ instead of $-A(t_0)$. Δt_D can be extracted from the measured data by computing the difference between the measured streaking angle and the one calculated assuming instantaneous tunneling.

A measurement of tunneling delay time was initially carried out for helium atoms employing 5.5-fs, elliptically polarized ($\varepsilon = 0.88$) near-IR pulses with peak intensity ranging from 2.3×10^{14}–3.5×10^{14} W cm^{-2} (6). For these intensities, the Keldysh parameter γ, defined as (64)

$$\gamma = \frac{\omega\sqrt{2I_p}}{E}, \tag{3}$$

where I_p is the ionization potential (24.59 eV for helium), ω is the laser center frequency, and E is the electric field amplitude, ranges between 1.45 and 1.17. According to the present terminology the experiment was performed in the so-called nonadiabatic tunneling regime (74). The result is consistent with an almost instantaneous tunneling delay time, yielding an intensity-averaged upper limit as small as 12 as (6). These experiments were then extended to much higher intensities

corresponding to a Keldysh parameter of 0.5 for He with an outcome that confirmed the earlier conclusion (75).

The first experiments also demonstrated how important it is to include the effect of the Coulomb force between the electron and the parent ion during the streaking process in the simulations. Even though the traditional strong-field physics approach of neglecting the interaction of electron and ion after ionization is very successful for many purposes, many examples have been reported revealing that the Coulomb force influences the electron trajectory in the continuum (76–78) or even below the barrier (79). This is true for any kind of experiment based on streaking.

For the particular case of attosecond angular streaking, the effect of the Coulomb field of the ion is a rotation of the whole distribution by an angle that depends on intensity. If this effect is not included in the simulated electron momentum distributions, wrong answers may be obtained as the angle is the primary observable in attoclock experiments. Neglecting the additional 7° of rotation observed in the streaking angle would lead to the wrong conclusion of a possible 50-as tunneling delay time.

Besides providing timing information, the attoclock actually offers the unique opportunity to study the influence of the Coulomb correction thanks to employing close-to-circularly polarized pulses (75). Linear polarization can lead to multiple returns of the electron to the core, whereas the close-to-circular polarization avoids rescattering (80). Any deviation from the electron kinematics driven by the laser field can thus be attributed directly to the potential. By monitoring the evolution of the additional offset to the streaking angle θ resulting from the Coulomb correction as a function of laser intensity for both helium and argon, it was shown that it is possible to obtain experimental information about the potential landscape experienced by the electron during and after tunneling as well as the exact tunneling exit point (75). Together with the estimations of the tunneling time and rate, the determination of the correct tunnel geometry helps to complete the picture of strong-field tunneling ionization.

For target atoms and ions with higher polarizability than helium, additional corrections have to be included in the semiclassical model; namely, Stark shift (81, 82) and multielectron effects become important under such circumstances. Both effects thus become more evident for argon than for helium, as can be seen in **Figure 5**.

Another key consideration is that the exit point of the electron after tunneling has to be calculated in parabolic coordinates, which separate the Schrödinger equation for the electron in the combined Coulomb and laser potentials (83). In the parabolic-separated problem, the tunneling process remains one-dimensional as in the more traditional approach based on Cartesian coordinates (33) (the field-direction model shown in **Figure 5**), because tunneling is allowed along one direction only (84). However, in the field-direction model, the problem does not separate and the electron is generally treated as a free particle in the transverse direction, an approximation not made in the approach using parabolic coordinates. The effective potential obtained along the parabolic coordinate through which tunneling occurs presents an additional term that affects both the location of the tunnel exit and the subsequent classical propagation. The corrected model describes the observed attosecond ionization dynamics also found in systems with higher polarizability. It is referred to as tunnel ionization in parabolic coordinates with induced dipole and Stark shift (75).

A recent study including these corrections to the semiclassical model confirmed the previously published (6) result of no measurable tunneling delay time with data taken over a larger intensity interval (75). The Keldysh parameter ranged from ~0.5 to 1.1 (1.4) for helium (argon).

The main conclusion from this application of the attoclock technique to very fundamental physics is twofold. First, the ion-electron interaction must be considered to prevent drawing the wrong conclusions on possible time delays in streaking measurements. Second, multielectron

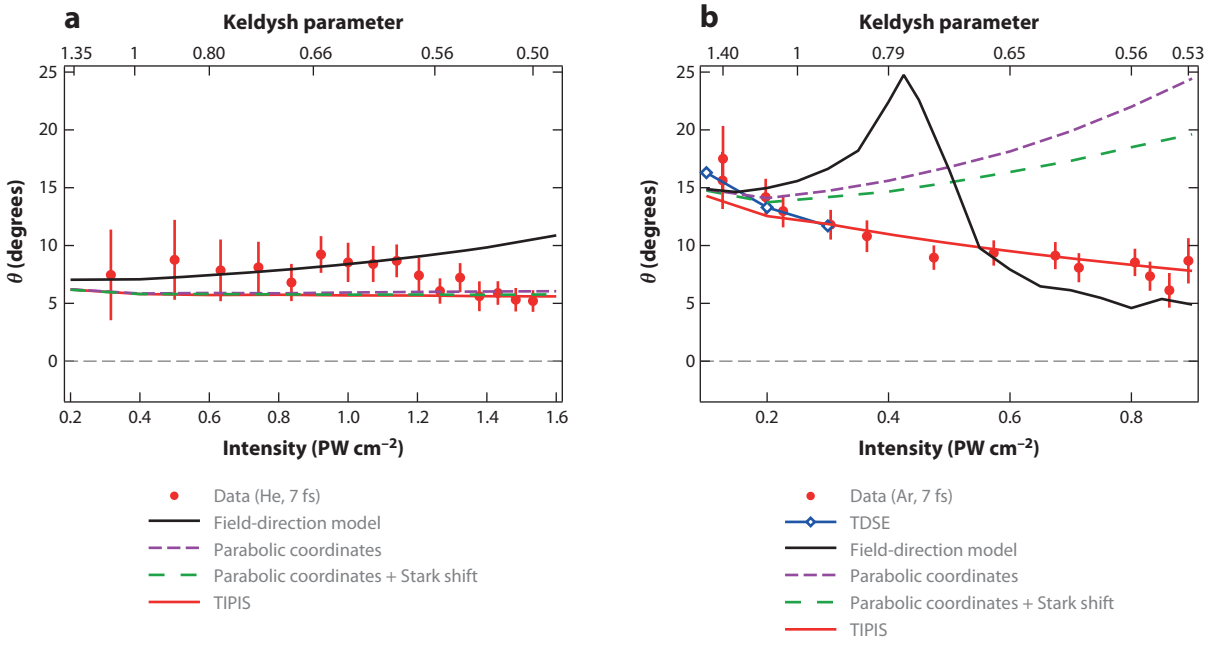

Figure 5

Tunnel ionization in parabolic coordinates with induced dipole and Stark shift model (TIPIS) to describe the interaction between liberated electron and parent ion. This interaction (which includes the Coulomb interaction) gives an angular correction to the streaking in the attoclock. (*a*) Experimental data of θ, obtained from ion momentum distributions in helium, together with the curves predicted by the semiclassical model with different assumptions. (*b*) Experimental data of θ, obtained from electron momentum distributions in argon, together with the curves predicted by the time-dependent Schroedinger equation (TDSE) and the semiclassical model with different assumptions. This clearly shows that multielectron effects need to be taken into account even for argon. At this point these multielectron contributions can be fully explained by their static parameters, which means that they occur on a sub-10-as timescale.

effects must be taken into account for a correct description of single-ionization—even with nearly circular polarized light. In recent years, many reports about observations that go beyond the traditional single active electron approximation have appeared, either in high-harmonic spectroscopy (85) or in photoionization (86, 87).

4.3. Electron Correlations in Double Ionization

Multielectron dynamics can be probed more directly by performing strong-field double ionization experiments. It is widely accepted that recollision of the first emitted electron with the parent ion is the dominating mechanism responsible for double ionization with linearly polarized fields (88, 89). However, with close-to-circular polarized light, where recollision does not occur, it is generally assumed that the two electrons can be treated independently and their ionization is solely laser-assisted (90).

Making full use of the attoclock, the ionization time could be extracted from the electron momentum distributions on two different timescales: a coarse scale following the pulse envelope that varies slowly with time (the "hour hand" of the attoclock) and a fine scale determined by the rapidly rotating electric-field vector (the "minute hand" of the attoclock, offering subfemtosecond resolution) (91). In terms of the geometry of the angular distribution of the electron momentum, the minute hand provides the angle-to-time mapping, whereas the hour hand results via the

magnitude of the electron momentum in a momentum-to-time mapping, similar to the attosecond streak camera (Section 2.1).

It is found that the second electron is released earlier than predicted by a model based on the assumption of two independent and successive release steps, whereas the ionization time of the first electron is in excellent agreement with the simulations. These conclusions are a strong indication that other electron correlation mechanisms besides recollision may be an important ingredient of strong-field double ionization. This process is not easily accessible on the basis of quantum mechanical models, because of exceedingly large computational complexity (92).

5. CONCLUSION AND OUTLOOK

As the examples in this review clearly illustrate, it is an ongoing trend in attosecond science to explore more and more fundamental questions. Whereas the early experiments mainly studied problems for which the answers were known beforehand, recent data show surprising and sometimes even puzzling results. We are now able to question assumptions that have proved to be very successful in atomic, molecular, and in particular, strong-field physics. When can a process be considered instantaneous, and when can it be treated in a single active electron approximation? As the field pushes the frontier to extreme timescales, subtle effects start to play a significant role in the interpretation of experiments that have traditionally not been accounted for. These experiments challenge the theoreticians to develop increasingly sophisticated models to improve the understanding of processes in the attosecond domain.

At the same time, new measurement techniques are being developed to address new questions or to reduce their experimental complexity and thereby broaden the scope and community for attosecond science. The attoclock is an example where a method was found to achieve attosecond resolution without requiring the difficult-to-generate attosecond pulses, whereas attosecond transient absorption enables probing observables that were inaccessible with previous tools.

It is expected that the trend for studying basic problems in physics and chemistry will continue for many more years. At the same time, however, the field will expand to more complex systems. First experiments on solid-state systems have been performed (11), but considerably more is expected to come in future. A wide area of interest is charge migration and coupling between layers of adsorbed molecules and their substrate. For example, it was found that excitation and emission of electrons from a negative-electron-affinity diamondoid monolayer on a noble metal surface takes place on a much faster timescale than can be resolved with traditional femtosecond techniques (93). A large range of systems exhibiting similarly fast dynamics is expected to emerge. Another area of interest is charge and energy transport in molecules (7). With the maturing of the experimental and theoretical tools in attosecond science, larger molecules become accessible to research on these timescales.

A strong focus on the technological side beyond the development of new spectroscopic tools is on the attosecond sources themselves. Scaling the generating laser fields to longer wavelengths is not only of interest for improving our understanding of the underlying strong-field physics (94, 95). At the expense of conversion efficiency, HHG photon energies scale with the wavelength squared (96). This enables extending attosecond pulse sources into the hundreds of electron volts and possibly even the low kilovolt range (97, 98), thereby approaching the M-absorption edges of important materials such as Fe, Ni, or Co. At the same time, it is crucial to further increase the attosecond pulse energies from the present state-of-the-art of a few nanojoules (41). This will ultimately enable true attosecond pump–attosecond probe experiments. Furthermore, the pulse repetition rate needs to be increased into the megahertz regime for improved signal-to-noise and reduced space charge effects (42, 99).

Attosecond pulses with even higher pulse and photon energies are expected from free-electron lasers (FELs) in the not-so-distant future (100–103). These sources will provide extremely high X-ray intensities at multikilovolt photon energies, enabling nonlinear optics with X-rays. Simultaneous attosecond temporal and Ångström spatial resolution are within reach with X-ray FELs (104–106). In contrast to everything else discussed in this review, FELs are large-scale facilities. Laser-driven undulator sources could become a promising lab-sized alternative filling the gap between the tabletop HHG-based systems and FELs (107). They replace the long linear accelerator of a FEL with a laser-plasma accelerator.

The first decade of attosecond science demonstrated the unique capabilities of the tools it provides. As we progress into its next decade, we observe how the field gains in depth by addressing increasingly fundamental questions and how it widens its scope to increasingly complex systems. This development is still strongly technology-driven. As new technology and methods open new doors, there is hardly any doubt that attosecond science will significantly expand its impact beyond its own realm into other branches of physics, chemistry, and possibly even biology.

SUMMARY POINTS

1. Attosecond science studies primarily electronic motion and energy transport on atomic and molecular scales.
2. In recent years, new spectroscopic tools in attosecond science have emerged. The attoclock achieves attosecond temporal resolution without using attosecond pulses, whereas attosecond transient absorption is an all-optical approach capable of probing previously inaccessible observables of a system.
3. Studying the dynamics of ionization processes is a major research focus in attosecond science and of fundamental interest to physics in general.
4. Measurements with the attoclock of the dynamics of strong-field tunnel ionization indicate that this process occurs instantaneously.
5. Two independent research groups report experiments on the delay in photoemission from different atomic energy levels. Both groups measure a finite delay on the order of tens of attoseconds.
6. Analysis of the experiments on the timing of ionization events shows that subtle effects start to play an important role on attosecond timescales; namely, the influence of the laser field used for measurement and multielectron effects cannot be neglected.

FUTURE ISSUES

1. Fundamental processes in physics and chemistry will remain a focus of attosecond science. These experiments will allow the refinement of our understanding of atomic and molecular processes in strong laser fields.
2. New spectroscopic tools and the maturing of the established methods enable attosecond science to advance toward more complex solid-state and molecular systems.
3. Wavelength scaling of the laser field generating the attosecond pulses extends the range of photon energies covered by attosecond techniques. Multihundred electron volts are within reach.

4. Energy scaling of the attosecond pulse sources brings us within reach of true attosecond pump–attosecond probe experiments.
5. FEL and laser-plasma undulator sources hold promise to push attosecond science into the multikilovolt photon energy regime.
6. As attosecond science approaches new frontiers, the need for new theoretical tools and concepts becomes apparent in certain areas of this strongly experiment-driven field.

DISCLOSURE STATEMENT

The authors are not aware of any affiliations, memberships, funding, or financial holdings that might be perceived as affecting the objectivity of this review.

ACKNOWLEDGMENTS

Our research presented in this review was supported by the National Centre of Competence in Research (NCCR) Quantum Photonics and NCCR Molecular Ultrafast Science and Technology, research instruments of the Swiss National Science Foundation.

LITERATURE CITED

1. Paul PM, Toma ES, Breger P, Mullot G, Augé F, et al. 2001. Observation of a train of attosecond pulses from high harmonic generation. *Science* 292:1689–92
2. Hentschel M, Kienberger R, Spielmann C, Reider GA, Milosevic N, et al. 2001. Attosecond metrology. *Nature* 414:509–13
3. Zewail AH. 2000. Femtochemistry: atomic-scale dynamics of chemical bond. *J. Phys. Chem. A* 104:5660–94
4. **Schultze M, Fiess M, Karpowicz N, Gagnon J, Korbman M, et al. 2010. Delay in photoemission. *Science* 328:1658–62**
5. Klünder K, Dahlström JM, Gisselbrecht M, Fordell T, Swoboda M, et al. 2011. Probing single-photon ionization on the attosecond time scale. *Phys. Rev. Lett.* 106:143002
6. **Eckle P, Pfeiffer A, Cirelli C, Staudte A, Dörner R, et al. 2008. Attosecond ionization and tunneling delay time measurements in helium. *Science* 322:1525–29**
7. Remacle F, Levine RD. 2006. An electronic time scale in chemistry. *Proc. Natl. Acad. Sci. USA* 103:6793–98
8. Drescher M, Hentschel M, Kienberger R, Uiberacker M, Yakovlev V, et al. 2002. Time-resolved atomic inner-shell spectroscopy. *Nature* 419:803–7
9. Goulielmakis E, Uiberacker M, Kienberger R, Baltuska A, Yakovlev V, et al. 2004. Direct measurement of light waves. *Science* 305:1267–69
10. Uiberacker M, Uphues T, Schultze M, Verhoef AJ, Yakovlev V, et al. 2007. Attosecond real-time observation of electron tunnelling in atoms. *Nature* 446:627–32
11. **Cavalieri AL, Müller N, Uphues T, Yakovlev VS, Baltuska A, et al. 2007. Attosecond spectroscopy in condensed matter. *Nature* 449:1029–32**
12. Föhlisch A, Feulner P, Hennies F, Fink A, Menzel D, et al. 2005. Direct observation of electron dynamics in the attosecond domain. *Nature* 436:373–76
13. Eckle P, Smolarski M, Schlup P, Biegert J, Staudte A, et al. 2008. Attosecond angular streaking. *Nat. Phys.* 4:565–70
14. Baker S, Robinson JS, Haworth CA, Teng H, Smith RA, et al. 2006. Probing proton dynamics in molecules on an attosecond time scale. *Science* 312:424–27

4. Measurement of ~20-as time delay in photoemission from 2p and 2s orbitals in neon.

6. Application of attoclock to measurement of tunneling delay time in tunnel ionization of helium.

11. First attosecond time-resolved experiment on a solid-state system.

15. Remetter T, Johnsson P, Mauritsson J, Varju K, Ni Y, et al. 2006. Attosecond electron wave packet interferometry. *Nat. Phys.* 2:323–26

16. Agostini P, DiMauro LF. 2004. The physics of attosecond light pulses. *Rep. Prog. Phys.* 67:813–55
17. Scrinzi A, Ivanov MY, Kienberger R, Villeneuve DM. 2006. Attosecond physics. *J. Phys. B* 39:1–37
18. Niikura H, Corkum PB. 2007. Attosecond and Angstrom science. *Adv. At. Mol. Opt. Phys.* 54:511–48
19. Corkum PB, Krausz F. 2007. Attosecond science. *Nat. Phys.* 3:381–87
20. Pfeifer T, Abel MJ, Nagel PM, Jullien A, Loh Z-H, et al. 2008. Time-resolved spectroscopy of attosecond quantum dynamics. *Chem. Phys. Lett.* 463:11–24
21. Kling MF, Vrakking MJJ. 2008. Attosecond electron dynamics. *Annu. Rev. Phys. Chem.* 59:463–92
22. Krausz F, Ivanov M. 2009. Attosecond physics. *Rev. Mod. Phys.* 81:163–234

23. Goulielmakis E, Loh Z-H, Wirth A, Santra R, Rohringer N, et al. 2010. Real-time observation of valence electron motion. *Nature* 466:739–43

24. Wang H, Chini M, Chen S, Zhang C-H, He F, et al. 2010. Attosecond time-resolved autoionization of argon. *Phys. Rev. Lett.* 105:143002

25. Holler M, Schapper F, Gallmann L, Keller U. 2011. Attosecond electron wave-packet interference observed by transient absorption. *Phys. Rev. Lett.* 106:123601

26. Pukhov A, Meyer-ter-Vehn J. 2002. Laser wake field acceleration: the highly non-linear broken-wave regime. *Appl. Phys. B* 74:355–61
27. Naumova N, Sokolov I, Nees J, Maksimchuk A, Yanovsky V, Mourou G. 2004. Attosecond electron bunches. *Phys. Rev. Lett.* 93:195003
28. Mikhailova YM, Platonenko VT, Rykovanov SG. 2005. Generation of an attosecond X-ray pulse in a thin film irradiated by an ultrashort ultrarelativistic laser pulse. *JETP Lett.* 81:571–74
29. Ferray M, L'Huillier A, Li XF, Lompré LA, Mainfray G, Manus C. 1988. Multiple-harmonic conversion of 1064 nm radiation in rare gases. *J. Phys. B* 21:L31–35
30. McPherson A, Gibson G, Jara H, Johann U, Luk TS, et al. 1987. Studies of multiphoton production of vacuum-ultraviolet radiation in the rare gases. *J. Opt. Soc. Am. B* 4:595–601
31. Krause JL, Schafer KJ, Kulander KC. 1992. Calculation of photoemission from atoms subject to intense laser fields. *Phys. Rev. A* 45:4998–5010
32. Krause JL, Schafer KJ, Kulander KC. 1992. High-order harmonic generation from atoms and ions in the high intensity regime. *Phys. Rev. Lett.* 68:3535–38
33. Corkum PB. 1993. Plasma perspective on strong-field multiphoton ionization. *Phys. Rev. Lett.* 71:1994–97
34. Lewenstein M, Balcou Ph, Ivanov MY, L'Huillier A, Corkum PB. 1994. Theory of high-harmonic generation by low-frequency laser fields. *Phys. Rev. A* 49:2117–32
35. Goulielmakis E, Schultze M, Hofstetter M, Yakovlev VS, Gagnon J, et al. 2008. Single-cycle nonlinear optics. *Science* 320:1614–17
36. Sola IJ, Mével E, Elouga L, Constant E, Strelkov V, et al. 2006. Controlling attosecond electron dynamics by phase-stabilized polarization gating. *Nat. Phys.* 2:319–22
37. Sansone G, Benedetti E, Calegari F, Vozzi C, Avaldi L, et al. 2006. Isolated single-cycle attosecond pulses. *Science* 314:443–46

38. Feng XM, Gilbertson S, Mashiko H, Wang H, Khan SD, et al. 2009. Generation of isolated attosecond pulses with 20 to 28 femtosecond lasers. *Phys. Rev. Lett.* 103:183901

39. Abel MJ, Pfeifer T, Nagel PM, Boutu W, Bell MJ, et al. 2009. Isolated attosecond pulses from ionization gating of high-harmonic emission. *Chem. Phys.* 366:9–14
40. Thomann I, Bahabad A, Liu X, Trebino R, Murnane MM, Kapteyn HC. 2009. Characterizing isolated attosecond pulses from hollow-core waveguides using multi-cycle driving pulses. *Opt. Exp.* 17:4611–33

41. Ferrari F, Calegari F, Lucchini M, Vozzi C, Stagira S, et al. 2010. High-energy isolated attosecond pulses generated by above-saturation few-cycle fields. *Nat. Photonics* 4:875–79

42. Keller U. 2010. Femtosecond to attosecond optics. *IEEE Photonics J.* 2:225–28
43. Itatani J, Quéré F, Yudin GL, Ivanov MY, Krausz F, Corkum PB. 2002. Attosecond streak camera. *Phys. Rev. Lett.* 88:173903

15. Interference of electron wave packets excited by subsequent pulses in an attosecond pulse train reveals quantum mechanical phase information.

23. First demonstration of attosecond transient absorption spectroscopy using isolated attosecond pulses.

25. First demonstration of attosecond transient absorption spectroscopy using attosecond pulse trains and resolving subfemtosecond dynamics.

38. Generation of isolated attosecond pulses from long (20–28 fs) infrared laser pulses.

41. Isolated attosecond pulses with nanojoule pulse energy.

44. Muller HG. 2002. Reconstruction of attosecond harmonic beating by interference of two-photon transitions. *Appl. Phys. B* 74:S17–21
45. Mauritsson J, Johnsson P, Mansten E, Swoboda M, Ruchon T, et al. 2008. Coherent electron scattering captured by an attosecond quantum stroboscope. *Phys. Rev. Lett.* 100:073003
46. Boutu W, Haessler S, Merdji H, Breger P, Waters G, et al. 2008. Coherent control of attosecond emission from aligned molecules. *Nat. Phys.* 4:545–49
47. Haessler S, Fabre B, Higuet J, Caillat J, Ruchon T, et al. 2009. Phase-resolved attosecond near-threshold photoionization of molecular nitrogen. *Phys. Rev. A* 80:011404
48. Haessler S, Caillat J, Boutu W, Giovanetti-Teixeira C, Ruchon T, et al. 2010. Attosecond imaging of molecular electronic wavepackets. *Nat. Phys.* 6:200–6
49. Telle HR, Steinmeyer G, Dunlop AE, Stenger J, Sutter DH, Keller U. 1999. Carrier-envelope offset phase control: a novel concept for absolute optical frequency measurement and ultrashort pulse generation. *Appl. Phys. B* 69:327–32
50. Dietrich P, Krausz F, Corkum PB. 2000. Determining the absolute phase of a few-cycle laser pulse. *Opt. Lett.* 25:16–18
51. Perelomov AM, Popov VS, Terentev MV. 1966. Ionization of atoms in an alternating electric field. *Zh. Eksp. Teor. Fiz.* 50:1393
52. Dörner R, Mergel V, Jagutzki O, Spielberger L, Ullrich J, et al. 2000. Cold target recoil ion momentum spectroscopy: a 'momentum microscope' to view atomic collision dynamics. *Phys. Rep.* 330:95–192
53. Smolarski M, Eckle P, Keller U, Dörner R. 2010. Semiclassical model for attosecond angular streaking. *Opt. Exp.* 18:17640–50
54. Gaarde MB, Buth C, Tate JL, Schafer KJ. 2011. Transient absorption and reshaping of ultrafast XUV light by laser-dressed helium. *Phys. Rev. A* 83:013419
55. Santra R, Yakovlev VS, Pfeifer T, Loh Z-H. 2011. Theory of attosecond transient absorption spectroscopy of strong-field-generated ions. *Phys. Rev. A* 83:033405
56. Loh Z-H, Khalil M, Correa RE, Santra R, Buth C, Leone SR. 2007. Quantum state-resolved probing of strong-field-ionized xenon atoms using femtosecond high-order harmonic transient absorption spectroscopy. *Phys. Rev. Lett.* 98:143601
57. Loh Z-H, Greene CH, Leone SR. 2008. Femtosecond induced transparency and absorption in the extreme ultraviolet by coherent coupling of the He 2s2p ($^1P^o$) and $2p^2$ ($^1S^e$) double excitation states with 800 nm light. *Chem. Phys.* 350:7–13
58. Johnsson P, Mauritsson J, Remetter T, L'Huillier A, Schafer KJ. 2007. Attosecond control of ionization by wave-packet interference. *Phys. Rev. Lett.* 99:233001
59. Lewenstein M, Salières P, L'Huillier A. 1995. Phase of the atomic polarization in high-order harmonic generation. *Phys. Rev. A* 52:4747–54
60. Salières P, Carré B, Déroff LL, Grasborn F, Paulus GG, et al. 2001. Feynman's path-integral approach for intense-laser-atom interactions. *Science* 292:902–5
61. Rivière P, Uhden O, Saalmann U, Rost JM. 2009. Strong field dynamics with ultrashort electron wave packet replicas. *New J. Phys.* 11:053011
62. Tong XM, Ranitovic P, Cocke CL, Toshima N. 2010. Mechanisms of infrared-laser-assisted atomic ionization by attosecond pules. *Phys. Rev. A* 81:021404
63. Jurvansuu M, Kivimäki A, Aksela S. 2001. Inherent lifetime widths of Ar $2p^{-1}$, Kr $3d^{-1}$, Xe $3d^{-1}$, and Xe $4d^{-1}$ states. *Phys. Rev. A* 64:012502
64. Keldysh LV. 1965. Ionization in the field of a strong electromagnetic wave. *Sov. Phys. JETP* 20:1307–14
65. Baggesen JC, Madsen LB. 2008. Theory for time-resolved measurements of laser-induced electron emission from metal surfaces. *Phys. Rev. A* 78:032903
66. Mairesse Y, Quéré F. 2005. Frequency-resolved optical gating for complete reconstruction of attosecond bursts. *Phys. Rev. A* 71:011401
67. Baggesen JC, Madsen LB. 2010. Polarization effects in attosecond photoelectron spectroscopy. *Phys. Rev. Lett.* 104:043602
68. Baggesen JC, Madsen LB. 2010. Polarization effects in attosecond photoelectron spectroscopy. *Phys. Rev. Lett.* 104:043602. Erratum. 2010. *Phys. Rev. Lett.* 104:209903

69. Zhang CH, Thumm U. 2010. Electron-ion interaction effects in attosecond time-resolved photoelectron spectra. *Phys. Rev. A* 82:043405
70. Nagele S, Pazourek R, Feist J, Doblhoff-Dier K, Lemell C, et al. 2011. Time-resolved photoemission by attosecond streaking: extraction of time information. *J. Phys. B* 44:081001
71. Paulus GG, Lindner F, Walther H, Baltuška A, Goulielmakis E, et al. 2003. Measurement of the phase of few-cycle laser pulses. *Phys. Rev. Lett.* 91:253004
72. Paulus GG, Grasborn F, Walther H, Villoresi P, Nisoli M, et al. 2001. Absolute-phase phenomena in photoionization with few-cycle laser pulses. *Nature* 414:182–84
73. Wittmann T, Horvath B, Helml W, Schätzel MG, Gu X, et al. 2009. Single-shot carrier–envelope phase measurement of few-cycle laser pulses. *Nat. Phys.* 5:357–62
74. Yudin GL, Ivanov MY. 2001. Nonadiabatic tunnel ionization: looking inside a laser cycle. *Phys. Rev. A* 64:013409
75. Pfeiffer AN, Cirelli C, Smolarski M, Dimitrovski D, Abu-samha M, et al. 2012. Attoclock reveals natural coordinates of the laser-induced tunneling current flow in atoms. *Nat. Phys.* 8:76–80
76. Blaga CI, Catoire F, Colosimo P, Paulus GG, Muller HG, et al. 2009. Strong-field photoionization revisited. *Nat. Phys.* 5:335–38
77. Liu CP, Hatsagortsyan KZ. 2010. Origin of unexpected low energy structure in photoelectron spectra induced by midinfrared strong laser fields. *Phys. Rev. Lett.* 105:113003
78. Goreslavski SP, Paulus GG, Popruzhenko SV, Shvetsov-Shilovski NI. 2004. Coulomb asymmetry in above-threshold ionization. *Phys. Rev. Lett.* 93:233002
79. Popruzhenko SV, Paulus GG, Bauer D. 2008. Coulomb-corrected quantum trajectories in strong-field ionization. *Phys. Rev. A* 77:053409
80. Dietrich P, Burnett NH, Ivanov M, Corkum PB. 1994. High-harmonic generation and correlated two-electron multiphoton ionization with elliptically polarized light. *Phys. Rev. A* 50:358588
81. Lein M. 2011. Streaking analysis of strong-field ionisation. *J. Mod. Opt.* 58:1188–94
82. Holmegaard L, Hansen JL, Kalhoj L, Kragh SL, Stapelfeldt H, et al. 2010. Photoelectron angular distributions from strong-field ionization of oriented molecules. *Nat. Phys.* 6:428–32
83. Landau LD, Lifschitz EM. 1958. *Quantum Mechanics: Non-Relativistic Theory*. New York: Oxford Univ. Press
84. Bisgaard CZ, Madsen LB. 2004. Tunneling ionization of atoms. *Am. J. Phys.* 72:249–54
85. Shiner AD, Schmidt BE, Trallero-Herrero C, Wörner HJ, Patchkovskii S, et al. 2011. Probing collective multi-electron dynamics in xenon with high-harmonic spectroscopy. *Nat. Phys.* 7:464–67
86. Litvinyuk IV, Legare F, Dooley PW, Villeneuve DM, Corkum PB, et al. 2005. Shakeup excitation during optical tunnel ionization. *Phys. Rev. Lett.* 94:033003
87. Walters ZB, Smirnova O. 2010. Attosecond correlation dynamics during electron tunnelling from molecules. *J. Phys. B* 43:161002
88. Weber T, Giessen H, Weckenbrock M, Urbasch G, Staudte A, et al. 2000. Correlated electron emission in multiphoton double ionization. *Nature* 405:658–61
89. Rudenko A, Zrost K, Feuerstein B, de Jesus VLB, Schroter CD, et al. 2004. Correlated multielectron dynamics in ultrafast laser pulse interactions with atoms. *Phys. Rev. Lett.* 93:253001
90. Maharjan CM, Alnaser AS, Tong XM, Ulrich B, Ranitovic P, et al. 2005. Momentum imaging of doubly charged ions of Ne and Ar in the sequential ionization region. *Phys. Rev. A* 72:041403
91. Pfeiffer AN, Cirelli C, Smolarski M, Dorner R, Keller U. 2011. Timing the release in sequential double ionization. *Nat. Phys.* 7:428–33
92. Becker W, Rottke H. 2008. Many-electron strong-field physics. *Contemp. Phys.* 49:199–223
93. Roth S, Leuenberger D, Osterwalder J, Dahl JE, Carlson RMK, et al. 2010. Negative-electron-affinity diamondoid monolayers as high-brilliance source for ultrashort electron pulses. *Chem. Phys. Lett.* 495:102–8
94. Colosimo P, Doumy G, Blaga CI, Wheeler J, Hauri C, et al. 2008. Scaling strong-field interactions towards the classical limit. *Nat. Phys.* 4:386–89
95. Doumy G, Wheeler J, Roedig C, Chirla R, Agostini P, DiMauro LF. 2009. Attosecond synchronization of high-order harmonics from midinfrared drivers. *Phys. Rev. Lett.* 102:093002
96. Tate J, Auguste T, Muller HG, Salières P, Agostini P, DiMauro LF. 2007. Scaling of wave-packet dynamics in an intense midinfrared field. *Phys. Rev. Lett.* 98:013901

97. Vozzi C, Calegari F, Frassetto F, Poletto L, Sansone G, et al. 2009. Coherent continuum generation above 100 eV driven by an IR parametric source in a two-color scheme. *Phys. Rev. A* 79:033842
98. Calegari F, Vozzi C, Negro M, Sansone G, Frassetto F, et al. 2009. Efficient continuum generation exceeding 200 eV by intense ultrashort two-color driver. *Opt. Lett.* 34:3125–27
99. Südmeyer T, Marchese SV, Hashimoto S, Baer CRE, Gingras G, et al. 2008. Femtosecond laser oscillators for high-field science. *Nat. Photonics* 2:599–604
100. Zholents AA, Fawley WM. 2004. Proposal for intense attosecond radiation from an X-ray free-electron laser. *Phys. Rev. Lett.* 92:224801
101. Zholents AA, Zolotorev MS. 2008. Attosecond X-ray pulses produced by ultra short transverse slicing via laser electron beam interaction. *New J. Phys.* 10:025005
102. Zholents A, Penn G. 2010. Obtaining two attosecond pulses for X-ray stimulated Raman spectroscopy. *Nucl. Instrum. Methods A* 612:254–59
103. Barletta WA, Bisognano J, Corlett JN, Emma P, Huang Z, et al. 2010. Free electron lasers: present status and future challenges. *Nucl. Instrum. Methods A* 618:69–96
104. Gaffney KJ, Chapman HN. 2007. Imaging atomic structure and dynamics with ultrafast X-ray scattering. *Science* 316:1444–48
105. Barty A, Boutet S, Bogan MJ, Hau-Riege S, Marchesini S, et al. 2008. Ultrafast single-shot diffraction imaging of nanoscale dynamics. *Nat. Photonics* 2:415–19
106. Marchesini S, Boutet S, Sakdinawat AE, Bogan MJ, Bajt S, et al. 2008. Massively parallel X-ray holography. *Nat. Photonics* 2:560–63
107. Fuchs M, Weingartner R, Popp A, Major Z, Becker S, et al. 2009. Laser-driven soft-X-ray undulator source. *Nat. Phys.* 5:826–29

Annual Review of
Physical Chemistry
Volume 63, 2012

Contents

Membrane Protein Structure and Dynamics from NMR Spectroscopy
Mei Hong, Yuan Zhang, and Fanghao Hu 1

The Polymer/Colloid Duality of Microgel Suspensions
L. Andrew Lyon and Alberto Fernandez-Nieves 25

Relativistic Effects in Chemistry: More Common Than You Thought
Pekka Pyykkö 45

Single-Molecule Surface-Enhanced Raman Spectroscopy
Eric C. Le Ru and Pablo G. Etchegoin 65

Singlet Nuclear Magnetic Resonance
Malcolm H. Levitt 89

Environmental Chemistry at Vapor/Water Interfaces: Insights from Vibrational Sum Frequency Generation Spectroscopy
Aaron M. Jubb, Wei Hua, and Heather C. Allen 107

Extensivity of Energy and Electronic and Vibrational Structure Methods for Crystals
So Hirata, Murat Keçeli, Yu-ya Ohnishi, Olaseni Sode, and Kiyoshi Yagi 131

The Physical Chemistry of Mass-Independent Isotope Effects and Their Observation in Nature
Mark H. Thiemens, Subrata Chakraborty, and Gerardo Dominguez 155

Computational Studies of Pressure, Temperature, and Surface Effects on the Structure and Thermodynamics of Confined Water
N. Giovambattista, P.J. Rossky, and P.G. Debenedetti 179

Orthogonal Intermolecular Interactions of CO Molecules on a One-Dimensional Substrate
Min Feng, Chungwei Lin, Jin Zhao, and Hrvoje Petek 201

Visualizing Cell Architecture and Molecular Location Using Soft X-Ray Tomography and Correlated Cryo-Light Microscopy
Gerry McDermott, Mark A. Le Gros, and Carolyn A. Larabell 225

Deterministic Assembly of Functional Nanostructures Using Nonuniform Electric Fields
Benjamin D. Smith, Theresa S. Mayer, and Christine D. Keating 241

Model Catalysts: Simulating the Complexities of Heterogeneous Catalysts
Feng Gao and D. Wayne Goodman 265

Progress in Time-Dependent Density-Functional Theory
M.E. Casida and M. Huix-Rotllant 287

Role of Conical Intersections in Molecular Spectroscopy and Photoinduced Chemical Dynamics
Wolfgang Domcke and David R. Yarkony 325

Nonlinear Light Scattering and Spectroscopy of Particles and Droplets in Liquids
Sylvie Roke and Grazia Gonella 353

Tip-Enhanced Raman Spectroscopy: Near-Fields Acting on a Few Molecules
Bruno Pettinger, Philip Schambach, Carlos J. Villagómez, and Nicola Scott 379

Progress in Modeling of Ion Effects at the Vapor/Water Interface
Roland R. Netz and Dominik Horinek 401

DEER Distance Measurements on Proteins
Gunnar Jeschke 419

Attosecond Science: Recent Highlights and Future Trends
Lukas Gallmann, Claudio Cirelli, and Ursula Keller 447

Chemistry and Composition of Atmospheric Aerosol Particles
Charles E. Kolb and Douglas R. Worsnop 471

Advanced Nanoemulsions
Michael M. Fryd and Thomas G. Mason 493

Live-Cell Super-Resolution Imaging with Synthetic Fluorophores
Sebastian van de Linde, Mike Heilemann, and Markus Sauer 519

Photochemical and Photoelectrochemical Reduction of CO_2
Bhupendra Kumar, Mark Llorente, Jesse Froehlich, Tram Dang, Aaron Sathrum, and Clifford P. Kubiak 541

Neurotrophin Signaling via Long-Distance Axonal Transport
Praveen D. Chowdary, Dung L. Che, and Bianxiao Cui 571

Photophysics of Fluorescent Probes for Single-Molecule Biophysics and Super-Resolution Imaging
Taekjip Ha and Philip Tinnefeld 595

Ultrathin Oxide Films on Metal Supports: Structure-Reactivity Relations
S. Shaikhutdinov and H.-J. Freund 619

Free-Electron Lasers: New Avenues in Molecular Physics and Photochemistry
Joachim Ullrich, Artem Rudenko, and Robert Moshammer 635

Dipolar Recoupling in Magic Angle Spinning Solid-State Nuclear Magnetic Resonance
Gaël De Paëpe 661

Indexes

Cumulative Index of Contributing Authors, Volumes 59–63 685

Cumulative Index of Chapter Titles, Volumes 59–63 688

Errata

An online log of corrections to Annual Review of Physical Chemistry chapters (if any, 1997 to the present) may be found at http://physchem.AnnualReviews.org/errata.shtml